

Er intercalation and its impact on transport properties of epitaxial graphene

Mingmin Yang(杨明敏), Yong Duan(端勇), Wenxia Kong(孔雯霞), Jinzhe Zhang(章晋哲), Jianxin Wang(王剑心), and Qun Cai(蔡群)

Citation: Chin. Phys. B, 2023, 32 (**6**): 066103. DOI: 10.1088/1674-1056/acbc6a
Journal homepage: http://cpb.iphy.ac.cn; http://iopscience.iop.org/cpb

What follows is a list of articles you may be interested in

Pressure-induced stable structures and physical properties of Sr-Ge system

Shuai Han(韩帅), Shuai Duan(段帅), Yun-Xian Liu(刘云仙), Chao Wang(王超), Xin Chen(陈欣), Hai-Rui Sun(孙海瑞), and Xiao-Bing Liu(刘晓兵)

Chin. Phys. B, 2023, 32 (**1**): 016101. DOI: 10.1088/1674-1056/ac6db5

Transition state and formation process of Stone—Wales defects in graphene

Jian-Hui Bai(白建会), Yin Yao(姚茵), and Ying-Zhao Jiang(姜英昭)

Chin. Phys. B, 2022, 31 (**3**): 036102. DOI: 10.1088/1674-1056/ac20c5

Highly tunable plasmon-induced transparency with Dirac semimetal metamaterials

Chunzhen Fan(范春珍), Peiwen Ren(任佩雯), Yuanlin Jia(贾渊琳), Shuangmei Zhu(朱双美), and Junqiao Wang(王俊俏)

Chin. Phys. B, 2021, 30 (**9**): 096103. DOI: 10.1088/1674-1056/abf4bf

Isostructural phase transition-induced bulk modulus multiplication in dopant-stabilized ZrO_2 solid solution

Min Wang(王敏), Wen-Shu Shen(沈文舒), Xiao-Dong Li(李晓东), Yan-Chun Li(李延春), Guo-Zhao Zhang(张国召), Cai-Long Liu(刘才龙), Lin Zhao(赵琳), Shu-Peng Lv(吕舒鹏), Chun-Xiao Gao(高春晓), Yong-Hao Han(韩永昊)

Chin. Phys. B, 2019, 28 (**7**): 076109. DOI: 10.1088/1674-1056/28/7/076109

Spectroscopic and scanning probe analysis on large-area epitaxial graphene grown under pressure of 4 mbar on 4H-SiC (0001) substrates

Wang Dang-Chao (王党朝), Zhang Yu-Ming (张玉明)

Chin. Phys. B, 2014, 23 (**7**): 076103. DOI: 10.1088/1674-1056/23/7/076103

Er intercalation and its impact on transport properties of epitaxial graphene

Mingmin Yang(杨明敏), Yong Duan(端勇), Wenxia Kong(孔雯霞),
Jinzhe Zhang(章晋哲), Jianxin Wang(王剑心), and Qun Cai(蔡群)†

State Key Laboratory of Surface Physics and Department of Physics, Fudan University, Shanghai 200433, *China*

(Received 31 October 2022; revised manuscript received 24 January 2023; accepted manuscript online 16 February 2023)

Intercalation of atomic species is a practicable method for epitaxial graphene to adjust the electronic band structure and to tune the coupling between graphene and SiC substrate. In this work, atomically flat epitaxial graphene is prepared on 4H-SiC(0001) using the flash heating method in an ultrahigh vacuum system. Scanning tunneling microscopy, Raman spectroscopy and electrical transport measurements are utilized to investigate surface morphological structures and transport properties of pristine and Er-intercalated epitaxial graphene. It is found that Er atoms are intercalated underneath the graphene layer after annealing at 900 °C, and the intercalation sites of Er atoms are located mainly at the buffer-layer/monolayer-graphene interface in monolayer domains. We also report the different behaviors of Er intercalation in monolayer and bilayer regions, and the experimental results show that the diffusion barrier for Er intercalated atoms in the buffer-layer /monolayer interface is at least 0.2 eV higher than that in the first/second graphene-layer interface. The appearance of Er atoms is found to have distinct impacts on the electronic transports of epitaxial graphene on SiC(0001).

Keywords: epitaxial graphene, intercalation, scanning tunneling microscopy (STM), electrical transport

PACS: 61.48.Gh, 68.37.Ef, 72.80.Vp, 68.37.–d **DOI:** 10.1088/1674-1056/acbc6a

As a two-dimensional material with honey-comb structure, graphene has aroused great interest due to its remarkable physical properties. Thermal decomposition of SiC is one of the most feasible routes to produce large-scale high-quality graphene. Epitaxial graphene (EG) on SiC substrate can be directly applied in semiconductor device without the need of any transfer. However, an electrically insulating buffer layer with $\left(6\sqrt{3}\times6\sqrt{3}\right)R30^\circ$ periodicity exists between EG and SiC substrate, about 30% carbon atoms of a buffer layer are covalently bound to the top Si atoms of SiC(0001) substrate.[1] The influence of the covalent bonding is a possible contributing factor to the reduced carrier mobility in EG as compared to exfoliated graphene. Intercalation of atomic species has shown to be a practicable way to tune the coupling between graphene and SiC substrate. Previous studies of graphene intercalation have focused on atoms with small atomic number, such as H,[1–5] Li,[6] Si,[7] and Cu.[8] Intercalations of rare-earth metal atoms or heavier atoms are rarely studied, only a few theoretical and experimental works about Au,[9,10] Bi,[11] Dy,[12] Yb,[12,13] and Eu[14] have been reported. Kim *et al.* showed that rare-earth metal intercalation is an efficient route to tune the electronic band structure of EG and will have potential applications.[12]

In order to find applications of graphene in spintronic devices and enhance its spin–orbit coupling, Bentley *et al.* have investigated Er intercalation in EG due to a high magnetic moment of Er atom (7 μ_B), and shown that Er atoms are intercalated underneath the buffer layer on 6H-SiC(0001) after annealing at 1000 °C.[15] Researchers have demonstrated that Er can react easily with Si and eventually form silicide.[16,17] We believe that Er atom growth can not only modify the electrical property of graphene, but also possibly reduce the temperature for EG fabrication, because of Si atom consumption by means of chemical combination with Er atoms at lower temperature.[18] In this work, erbium is selected as the intercalant for EG generated on a 4H-SiC(0001) substrate. Our experimental results show that the intercalation sites of Er atoms are located at the buffer-layer/monolayer-graphene interface, quite different from Bentley's results. We elucidate the different intercalation configurations of Er atoms on monolayer and bilayer domains of EG. It is also exhibited that the appearance of Er atoms can have distinct impacts on the electronic transports of EG on SiC(0001) surface. These results will provide the possibility to manipulate the electronic structures with different atoms intercalated into different atomic interfaces of EG.

Our experiments were performed in an Omicron ultrahigh vacuum (UHV) scanning tunneling microscopy (STM) system (pressure $\sim 2\times10^{-10}$ mbar). Large-scale EG on clean 4H-SiC(0001) substrate was prepared by means of flash heating. Flash heating includes the following steps: (i) Heat the 4H-SiC(0001) substrate at 650 °C for 330 s. (ii) Raise the temperature from 650 °C to 1350 °C in 30 s and keep temperature at 1350 °C for 60 s. (iii) Reduce the temperature back to 650 °C in 60 s. (iv) Repeat the above three steps for more than 200 times. After EG formation, Er atoms were evaporated onto

†Corresponding author. E-mail: qcai@fudan.edu.cn

© 2023 Chinese Physical Society and IOP Publishing Ltd

the EG/SiC samples at room temperature for 1 min–12 min, the deposition rate is 0.06 nm/min. Then the Er-decorated EG/SiC samples were annealed for several tens of minutes at 800 °C–1000 °C for Er intercalation. STM observations were carried out with electro-chemically etched W tips at room temperature. After STM imaging, samples were transferred out of UHV system for *ex situ* Raman spectroscopy and transport measurements. The Raman spectra were acquired by using a laser excitation of 532 nm at room temperature, and the laser spot size is ~ 5 μm. To investigate the electrical transport properties of EG, micron scale Hall-bars were patterned on the EG/SiC and Er/EG/SiC samples using electron beam lithography followed by the 10 nm/50 nm Cr/Au depositions and lift-off process. The transport measurements were conducted in an Evercool Ⅱ physical property measurement system (PPMS), with the temperature ranging from 2 K to 300 K.

Figure 1(a) shows wide terraces with almost regular edge of EG prepared by using flash heating, and the width of terrace is 200–300 nm. Monolayer and bilayer graphene (called MLG and BLG in the following, respectively) are found co-existing on the terraces. STM images prove that flash heating has significant advantages in realizing EG growth control about homogeneity, continuity, and number of layers. After Er intercalation at 900–1000 °C annealing, the STM image in Figs. 1(b) and 1(c) shows that many individual islands (diameter < 50 nm) never observed before are exhibited on the terrace. These small islands are probed with an apparent height larger than the height difference between MLG and BLG, with totally different surface morphological characteristics. Thus, the small islands are considered to be Er islands formed by intercalation process. The atomic resolution STM image obtained on the Er island (displayed in Fig. 1(d)) provides direct evidence. The honey-comb lattice of MLG can be seen spreading over the surface of Er island in the inset in Fig. 1(d), which confirms that Er islands are intercalated underneath the graphene layer, rather than located on the surface of graphene. It is quite interesting to find that almost all Er islands are distributed in monolayer region, even if they are very close to the boundary between MLG and BLG.

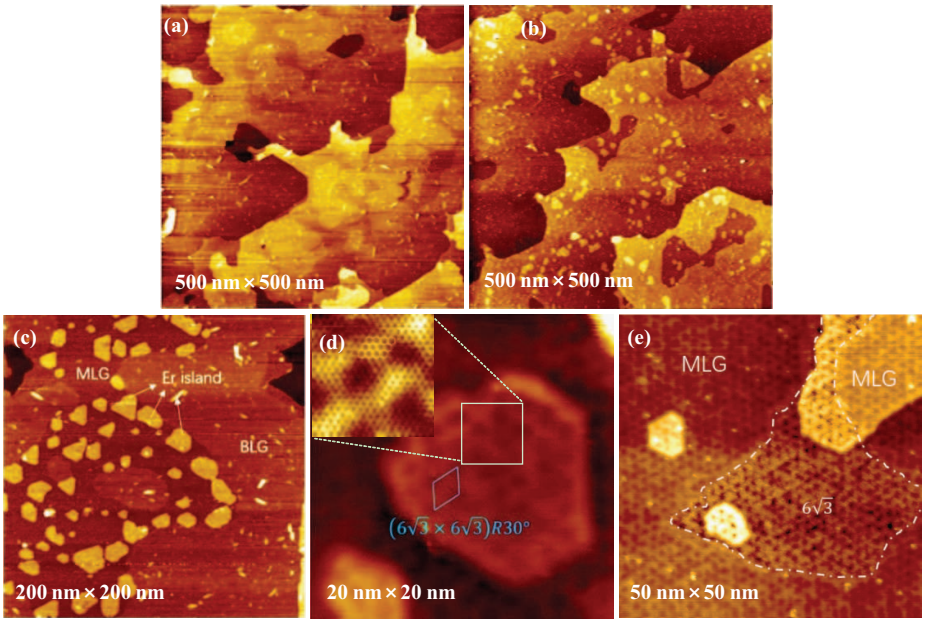


Fig. 1. STM images acquired on EG/SiC(0001) samples: (a) before Er intercalation ($V_{\rm bias} = 0.3$ V, $I_{\rm t} = 300$ pA), (b) after Er intercalation ($V_{\rm bias} = 0.3$ V, $I_{\rm t} = 300$ pA), (c) with coexisting monolayer graphene, bilayer graphene and Er islands ($V_{\rm bias} = 0.6$ V, $I_{\rm t} = 300$ pA), (d) with one Er island intercalated underneath monolayer graphene [$V_{\rm bias} = 0.3$ V, $I_{\rm t} = 400$ pA; inset in (d) is the atomic resolution image of monolayer graphene covered on top of the Er island with scanning area of 4 nm × 4 nm], (e) with three Er islands observed on the surface. The domain boundary between MLG and the buffer layer is marked by a white line.

Now the studies about Er intercalation are concentrated on determining the intercalation site of Er atoms. For the intercalation site in MLG region, there are two probabilities: one is the interface between MLG and the buffer layer, the other is that between the buffer layer and the SiC substrate. STM image in Fig. 1(d) shows that the contrast corrugation similar as that of $\left(6\sqrt{3}\times 6\sqrt{3}\right)R30°$ structure is clearly visible on Er island, with the same orientations as the $6\sqrt{3}$ structure observed in MLG around the island. As mentioned in previous works, the $6\sqrt{3}$ structure observed in graphene results from the influence of the buffer layer.[19,20] If Er atoms are intercalated between the buffer layer and the SiC substrate, the buffer layer will convert into a free-standing graphene layer, which is decoupled with the substrate and no longer shows $6\sqrt{3}$ reconstruction. In Fig. 1(e), three Er islands are detected on the surface, the left one is intercalated underneath MLG, another at the lower left is formed just on the top of the buffer layer, and the large island is partly covered by MLG at the right. These

STM images definitely demonstrate that, in MLG region, Er atoms are intercalated into the interface between MLG and the buffer layer. The same conclusion can be drawn from our intercalation experiments after annealing at 1000 °C even for 1–2 h. Using low energy electron diffraction and photoemission spectroscopy, Bentley *et al.* have found that annealing at 1000 °C results in Er intercalation into the interface between the buffer layer and the 6H-SiC(0001) substrate, with Er atoms evaporated onto the $6\sqrt{3}$/SiC samples.[15]

For BLG region, it is more complicated to make sure the intercalation site of Er atoms. In BLG area of Er-intercalated EG, some light dots are observed less than 1 nm, as highlighted in Fig. 2(a) with yellow circles. The zoom-in image in Fig. 2(b) indicates that these dots are actually particle-like protrusions, completely different from common defects in BLG and inexistent on pristine EG. These light dots are believed to be induced by Er atoms intercalated underneath graphene layer. At the same time, several light dots are also probed in MLG region in the lower right corner of Fig. 2(a). Intercalated Er atoms behave quite differently in MLG and BLG regions. In MLG, Er atoms are self-assembled mainly into nano-islands, and only a few light dots can be seen. In BLG region, Er atoms appear as light dots rather than nano-islands. More than 90% intercalated Er atoms are distributed in MLG region. These different distributions of intercalated Er atoms may be attributed to the different adsorption energies on graphene and buffer layer. For the $6\sqrt{3}$ buffer layer, there are many dangling bonds existing, but no dangling bond can be found on the perfect graphene layer. Hence, adsorption and nucleation of metal atoms take place preferentially on the buffer layer instead of graphene.[21] It is also found that the atoms grown on graphene domains can diffuse extraordinarily fast towards buffer layer regions because of the low diffusion barrier.[22,23]

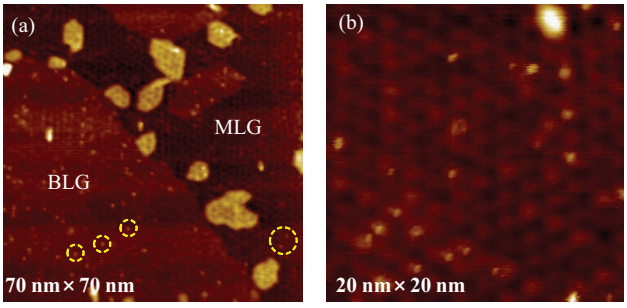


Fig. 2. (a) STM image of Er/EG/SiC(0001) obtained on a region including MLG and BLG. Er intercalated islands are found located mainly in MLG region ($V_{\rm bias} = -2.2$ V, $I_{\rm t} = 600$ pA). (b) Zoom-in image of light dots in BLG region ($V_{\rm bias} = -1.8$ V, $I_{\rm t} = 600$ pA).

For the case of bilayer region, three possible intercalation interfaces should be taken into account: one is between the two graphene layers, another is between the graphene layer and the buffer layer, the last one is between the buffer layer and the SiC substrate. If Er atoms are intercalated between the bottom graphene layer and the buffer layer, the dots induced by Er atoms should be covered by two graphene layers and randomly filled in the structural undulations of the buffer layer. The Er dots cannot be as bright and palpable as the dots shown in Fig. 2(b). The different intercalation behaviors of Er atoms in MLG and BLG also indicate that Er atoms in BLG cannot be intercalated into the same interface as in MLG. In addition, it is difficult for Er atoms in BLG to intercalate beneath the buffer layer by penetrating through three atomic layers during annealing. Effects of the confined space between graphene layers on atom diffusions have been manifested in bilayer EG,[24] suggesting that Er atoms in BLG region probably go through the top graphene and are intercalated into the interface between the two graphene layers.

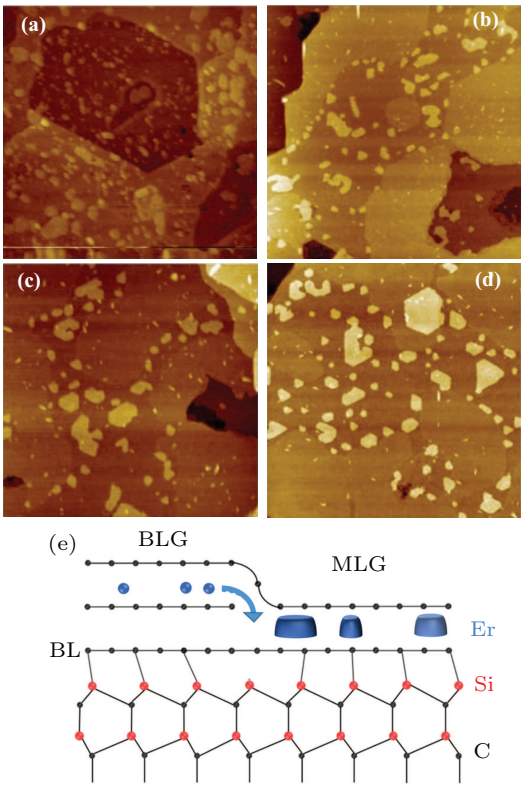


Fig. 3. STM images (200 nm × 200 nm) obtained on an Er/EG/SiC(0001) sample after (a) annealing at 800 °C for 10 min ($V_{\rm bias} = 0.3$ V, $I_{\rm t} = 400$ pA); (b) another annealing at 900 °C for 10 min ($V_{\rm bias} = 1.8$ V, $I_{\rm t} = 600$ pA); (c) further annealing at 1000 °C for 10 min ($V_{\rm bias} = 1.8$ V, $I_{\rm t} = 600$ pA); (d) annealing at 1000 °C for another 20 min ($V_{\rm bias} = 1.8$ V, $I_{\rm t} = 600$ pA); (e) schematic diagram of intercalated Er atoms diffusing from BLG to MLG and migrating to assemble into islands.

In the literature, three mechanisms of atom intercalations have been reported. The external atoms intercalate into graphene: (i) through the original defects of EG layer;[6,7] (ii) through the edges of graphene domains;[6] (iii) by inducing new defects in EG during annealing process.[25] The existing of defects on the EG sample provides the opportunity for Er atoms to intercalate graphene through original defects. If Er atoms are intercalated into EG only through the original defects, only a few light dots would be observed in Fig. 2(b). It

is obvious that in Fig. 2(b) few defects have been detected on the surface, insufficient for a number of Er atoms to intercalate through. Light dots are distributed randomly throughout the BLG region, showing no position dependence on the original defect sites. In our STM results, the number of defects on the graphene layer is also observed to increase after Er intercalation. Therefore, Er atoms are considered to intercalate into EG by inducing new defects in the graphene layer during annealing process. In addition, the intercalation through the edges of graphene domains can also be observed occasionally in our experiments, as substantiated by the STM image in Fig. 1(e) such that an island is found locating across the boundary between MLG and the buffer layer.

To observe the evolution process of Er intercalation in EG, one Er-evaporated EG sample has been annealed serially at different temperature for a few minutes. Figure 3 shows the STM images obtained on this sample after each annealing. Annealing at 800 °C for 10 min does not make the intercalation occur, as shown in Fig. 3(a), where large Er clusters are still distributed on the external surface of EG randomly. After another annealing at 900 °C for 10 min, the intercalation takes place and flat Er islands are found to intercalate underneath graphene (shown in Fig. 3(b)) and mainly distributed in MLG region. Many small islands reside on the MLG side along the boundary between MLG and BLG regions, implying that these Er islands consist of the atoms migrating primarily from BLG to MLG region. Figures 3(b)–3(d) exhibit that shapes of Er islands have a tendency to be more regular with annealing duration, transformed from irregular shapes with distorted border to regular ones with well-defined edges and same lattice orientations as graphene. With annealing treatments proceeding, the large compact islands increase in number while small islands are shrinking. It is indicated that Er atoms desorb from small islands, diffuse in the interfacial space, and congregate in large islands, illustrating an Ostwald ripening process.[26]

According to the experimental results, we propose a model for the process of intercalated Er atoms diffusing from BLG to MLG region and assembling into Er islands, as depicted in Fig. 3(e). At the beginning, Er atoms are deposited on EG surface uniformly. During annealing at 900 °C, Er atoms can be intercalated beneath a graphene layer chiefly by generating defects in both MLG and BLG regions. In MLG region, due to the higher diffusion barrier, Er intercalated atoms are easy to encounter each other and actualize stable nucleation, finally aggregate into various compact islands. In BLG region, intercalated Er atoms tend to migrate long distances resulting from the low barrier for diffusion. A large number of atoms can even migrate to the boundaries of MLG and BLG regions, then enter into MLG region. Only a few atoms remaining in BLG region are probed as light dots in STM images. Based on the size of BLG region, the diffusion length of Er intercalated atoms can be estimated as ~ 50 nm. In MLG, the diffusion length of the atoms is estimated to be ~ 20 nm according to the distribution of Er islands. Using expressions $x = \sqrt{Dt}$ and $D = D_0 \exp(-E/kT)$ for diffusion, we can obtain that the diffusion barrier for Er intercalated atoms in the interface between monolayer graphene and the buffer layer is at least 0.2 eV higher than that in the interface between the two graphene layers. We believe this is prompted by the existing of dangling bonds in the buffer layer and/or its bonding with the top Si atoms of the SiC(0001) substrate.

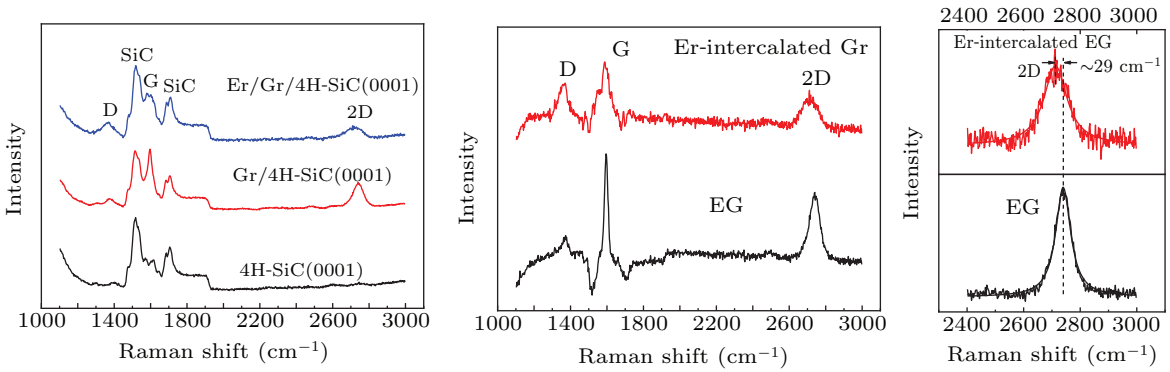


Fig. 4. (a) The original Raman spectra of SiC(0001) substrate, EG/SiC(0001) and Er/EG/SiC(0001). (b) Raman spectra of EG/SiC(0001) and Er/EG/SiC(0001) with the signal of SiC(0001) substrate subtracted. (c) The enlargements of the 2D peaks in (b). The solid lines are the fitted curves, indicating that the 2D peak can be fitted as a single Lorentz peak before and after Er intercalation.

Raman spectrum measurements have provided more information about Er intercalation in EG. Figure 4(a) depicts the Raman spectra acquired on pristine EG, Er-intercalated EG and the clean SiC(0001) substrate. The representative results of pristine EG and Er-intercalated EG show three graphene peaks (D peak at ~ 1350 cm^{-1}, G peak at ~ 1580 cm^{-1}, 2D peak at ~ 2700 cm^{-1}) and two SiC peaks (at ~ 1517 cm^{-1} and ~ 1709 cm^{-1}). The Raman spectra of EG on SiC always consist of a combination of signals from graphene and SiC. The Raman peaks of graphene and SiC can be separated by a simple subtraction of a SiC spectrum.[27–29] We plot the Raman signals from graphene in Fig. 4(b), which clearly exhibits

three typical Raman peaks for graphene on SiC: the D, G and 2D peaks. Usually, the full width at half maximum (FWHM) of 2D peak and the ratio of integrated intensity of 2D and G peaks (I_{2D}/I_G) are used to determine the number of graphene layers. For EG grown on SiC(0001), the FWHM of 2D peak are ~ 60 cm^{-1} for monolayer graphene and ~ 95 cm^{-1} for bilayer graphene, and the intensity of G peak is often larger than that of 2D peak.[30] Black line in Fig. 4(b) displays the Raman spectrum of pristine EG, with D peak at 1374 cm^{-1}, G peak at 1594 cm^{-1}, and 2D peak at 2740 cm^{-1}. The FWHM of 2D peak is 75.6 cm^{-1}, indicating that the pristine EG is composed of a mixture of monolayer and bilayer graphene, consistent with the STM observations.

After Er intercalation, the Raman spectrum [red line in in Fig. 4(b)] shows that the positions of G and D peaks almost have not changed, but 2D peak moves to 2711 cm^{-1}, with a red shift of 29 cm^{-1} which is usually attributed to electron/hole doping or strain effect.[31] The I_{2D}/I_G ratio decays to 0.57 from 0.74. Das *et al.* have manifested that I_{2D}/I_G ratio has a strong correlation with the doping concentration in graphene: I_{2D}/I_G ratio decreases with the increase of doping concentration.[32] The variation of 2D peak with doping is mainly due to charge transfer, with hole doping resulting in an upshift, and the opposite for high electron doping.[31] Therefore, the Raman results show that the intercalations of Er atoms make the doping concentration of electron increase in EG. The red shift of 2D peak results from the increase of electron doping concentration and conceivable strain relief in graphene layers induced by Er intercalation.[33] Furthermore, the FWHM of 2D peak is 90.2 cm^{-1} after Er intercalation, still between the values of monolayer and bilayer graphene. This proves the fact that Er atoms are not intercalated between the buffer layer and the SiC substrate, otherwise the number of graphene layers would be changed. It is also noticed that the I_D/I_G ratio increases to 0.71 from 0.13, and the FWHM of G peak becomes broader. Both changes indicate that more defects appear in EG, providing further evidence for Er atoms intercalated underneath the graphene layer.

Transport measurements of EG samples with and without Er intercalation have been conducted by using the PPMS. The Hall coefficients of EG before and after the intercalation are found to be negative, signifying an n-type conduction. As shown in Fig. 5, the carrier mobility μ decreases with the increase of temperature for both pristine EG and Er-intercalated EG, in agreement with other works reported.[2,34] The main reason for reduction of carrier mobility with temperature increasing is attributed to remote phonon scattering and the related phonon modes mainly come from the interface between the buffer layer and the SiC substrate.[2] When the stimulation current is 5 μA, the carrier mobility of our pristine EG decreases from 125.57 cm^2/V·s to 27.81 cm^2/V·s and that of the sample after Er intercalation decreases from 92.20 cm^2/V·s to 20.28 cm^2/V·s, with the temperature increasing from 6 K to 300 K, and these results may be connected with a higher electron density induced by Er intercalation. The decrease rate in carrier mobility before and after Er intercalation shows a trend of increasing at first and then declining at the same range of temperature, varying between 26% and 48%. The specific values of carrier mobility can be found in Table S1. The situation is similar for the excitation current of 50 μA. There is still a wide gap in carrier mobility between EG on SiC (with/without Er intercalation) and exfoliated graphene (even to 15000 cm^2/V·s), suggesting that the coupling between EG and the SiC substrate keeps nearly in the same state after Er intercalation. This also provides further evidence for Er intercalation at the interface above the $6\sqrt{3}$ buffer layer.

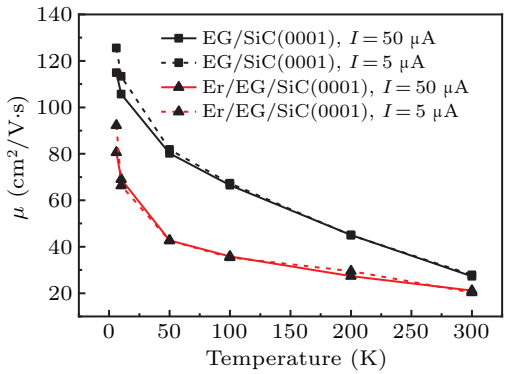


Fig. 5. The temperature dependence of carrier mobility μ of the EG/SiC(0001) and Er/EG/SiC(0001) samples obtained under stimulation currents of 50 μA and 5 μA, respectively.

In conclusion, the pristine and Er-intercalated EG grown on 4H-SiC(0001) substrates have been investigated using STM, Raman spectroscopy and transport measurements. The EG is detected as a mixture of monolayer and bilayer graphene on SiC. Er atoms start to intercalate beneath the graphene layer by means of annealing at 900 °C. STM observations show that intercalated Er atoms behave dissimilarly in MLG and BLG regions. Most Er intercalated atoms distribute in MLG region in the interface between the buffer layer and monolayer graphene, and assemble into compact islands, as confirmed by STM and Raman results. Only a few Er atoms are probed in BLG region as individual light dots which distribute in the interface between the two graphene layers. According to STM measurements, the diffusion barrier for Er intercalated atoms in the buffer-layer/monolayer interface is calculated at least 0.2 eV higher than that in the first/second graphene-layer interface. The results of Raman and transport measurements also demonstrate that Er intercalation makes the doping concentration of electron increase in EG and thus results in decrease of carrier mobility. These findings will pave the way to manipulate electronic structures with different atoms intercalated into different atomic interfaces of EG.

Acknowledgement

Project supported by the Natural Science Foundation of Shanghai Science and Technology Committee (Grant No. 18ZR1403300).

References

[1] Riedl C, Coletti C, Iwasaki T, *et al.* 2009 *Phys. Rev. Lett.* **103** 246804
[2] Speck.F, Jobst J, Fromm F, *et al.* 2011 *Appl. Phys. Lett.* **99** 122106
[3] Rajput S, Li Y Y and Li L 2014 *Appl. Phys. Lett.* **104** 041908
[4] Dharmaraj P, Justin Jesuraj P and Jeganathan K 2016 *Appl. Phys. Lett.* **108** 051605
[5] Forti S, Emtsev K V, Coletti C, *et al.* 2011 *Phys. Rev. B* **84** 125449
[6] Fiori S, Murata Y, Veronesi S, *et al.* 2017 *Phys. Rev. B* **96** 125429
[7] Xia C, Watcharinyanon S, Zakharov A A, *et al.* 2012 *Phys. Rev. B* **85** 045418
[8] Yagyu K, Tajiri T, Kohno A, *et al.* 2014 *Appl. Phys. Lett.* **104** 053115
[9] Marchenko D, Varykhalov A, Sánchez-Barriga J, *et al.* 2016 *Appl. Phys. Lett.* **108** 172405
[10] Premlal B, Cranney M, Vonau F, *et al.* 2009 *Appl. Phys. Lett.* **94** 263115
[11] Warmuth J, Bruix A, Michiardi M, *et al.* 2016 *Phys. Rev. B* **93** 165437
[12] Kim M, Tringides M C, Hershberger M T, *et al.* 2017 *Carbon* **123** 93
[13] Watcharinyanon S, Johansson L I, Xia C, *et al.* 2013 *Graphene* **2** 66
[14] Schumacher S, Huttmann F, Petrović M, *et al.* 2014 *Phys. Rev. B* **90** 235437
[15] Bentley P D, Bird T W, Graham A P J, *et al.* 2021 *AIP Adv.* **11** 025314
[16] Baglin J E, d'Heurle F M and Petersson C S 1980 *Appl. Phys. Lett.* **36** 594
[17] Chen G, Wan J, Yang J, *et al.* 2002 *Surf. Sci.* **513** 203
[18] Duan Y, Kong W X, Zhang J Z, *et al.* 2022 *J. Appl. Phys.* **132** 135701
[19] Varchon F, Mallet P, Veuillen J Y, *et al.* 2008 *Phys. Rev. B* **77** 235412
[20] Goler S, Coletti C, Piazza V, *et al.* 2013 *Carbon* **51** 249
[21] Hu T W, Ma F, Ma D Y, *et al.* 2013 *Appl. Phys. Lett.* **102** 171910
[22] Liu X J, Wang C Z, Hupalo M, *et al.* 2012 *Phys. Chem. Chem. Phys.* **14** 9157
[23] Liu X J, Wang C Z, Hupalo M, *et al.* 2013 *Crystals* **3** 79
[24] Wang W X, Wei Y W, Li S Y, *et al.* 2018 *Phys. Rev. B* **97** 085407
[25] Guo H, Lu H L, Huang L, *et al.* 2017 *Acta Phys. Sin.* **66** 216803 (in Chinese)
[26] Zhu Y, Zhou W, Wang S, *et al.* 2006 *J. Appl. Phys.* **100** 114312
[27] Kunc J, Hu Y, Palmer J, *et al.* 2013 *Appl. Phys. Lett.* **103** 201911
[28] de Heer W A, Berger C, Wu X, *et al.* 2010 *J. Phys. D: Appl. Phys.* **43** 374007
[29] Suemitsu M and Fukidome H 2010 *J. Phys. D: Appl. Phys.* **43** 374012
[30] Ni Z H, Chen W, Fan X F, *et al.* 2008 *Phys. Rev. B* **77** 115416
[31] Casiraghi C, Pisana S, Novoselov K S, *et al.* 2007 *Appl. Phys. Lett.* **91** 233108
[32] Das A, Pisana S, Chakraborty B, *et al.* 2008 *Nat. Nanotechnol.* **3** 210
[33] Schumacher S, Forster D F, Rosner M, *et al.* 2013 *Phys. Rev. Lett.* **110** 086111
[34] Yu C, Liu Q, Li J, *et al.* 2014 *Appl. Phys. Lett.* **105** 183105